Universiteit
Leiden
The Netherlands

Dynamics of the Oort cloud and formation of interstellar comets

Torres Rodriguez, S.

Citation
Torres Rodriguez, S. (2020, April 30). *Dynamics of the Oort cloud and formation of interstellar comets*. Retrieved from https://hdl.handle.net/1887/87515

Version:	Publisher's Version
License:	Licence agreement concerning inclusion of doctoral thesis in the Institutional Repository of the University of Leiden
Downloaded from:	https://hdl.handle.net/1887/87515

Note: To cite this publication please use the final published version (if applicable).

Cover Page

Universiteit Leiden

The handle http://hdl.handle.net/1887/87515 holds various files of this Leiden University dissertation.

Author: Torres Rodriguez, S.
Title: Dynamics of the Oort cloud and formation of interstellar comets
Issue Date: 2020-04-30

Credit: Science Photo Library

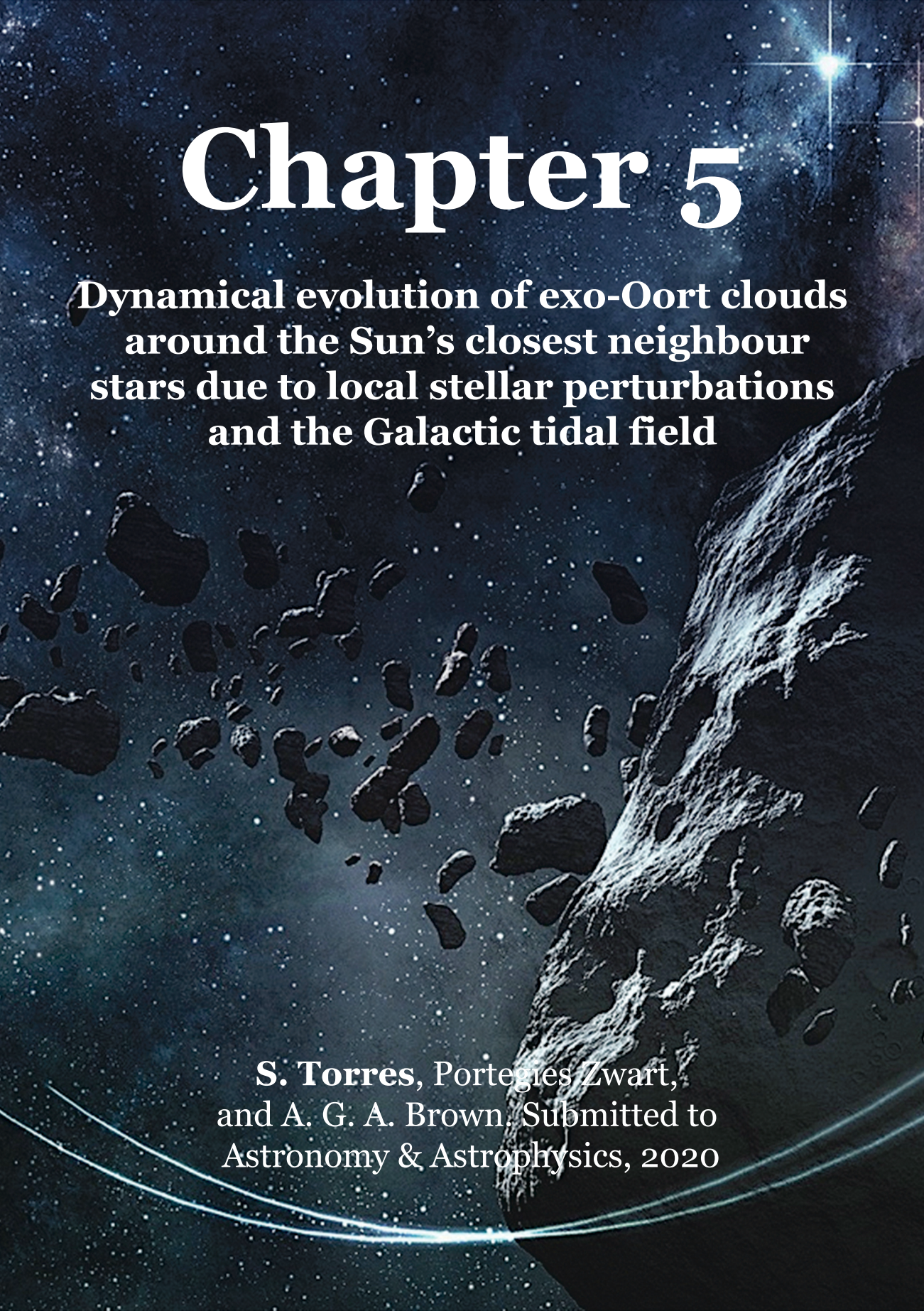

Chapter 5

Dynamical evolution of exo-Oort clouds around the Sun's closest neighbour stars due to local stellar perturbations and the Galactic tidal field

S. Torres, Portegies Zwart, and A. G. A. Brown. Submitted to Astronomy & Astrophysics, 2020

Abstract

The dynamical evolution of the outer Oort cloud in the solar system is affected by passing stars and the Galactic tidal field. These perturbations can strip comets from the cloud, forming *sōlī lapidēs* (interstellar objects). If we assume that the Sun's neighbour stars also have Oort cloud-like structures, and therefore undergo similar perturbations, interstellar comets are expected to be common in the local solar neighbourhood. In this work we investigate the dynamical evolution of comets in an exo-Oort cloud around the Sun's neighbour stars, accounting for the effect of passing stars and the Galactic tidal field. Using proper motions, parallaxes, and radial velocities from Gaia DR2, we studied a subset of the stars within 3 pc from the Sun, i.e., the systems: Proxima Centauri, Barnard's star, Gliese 65, Ross 154, and Ross 248. For each system, we then calculate the closest encounter with other stars they had in the last 10 Myr and will have in the next 10 Myr. We find that on average the stars in the local solar neighbourhood experiences around 40-55 encounters within 2.5pc from each star during 20 Myr, primarily with M-dwarfs stars. Using the Astrophysical Multipurpose Software Environment (AMUSE), and the GPU-accelerated direct N-body code ABIE, we then calculate the effect of passing stars and the Galactic tidal field on the comets in exo-Oort clouds around the Sun's neighbour stars. The most perturbed system is the binary system Gliese 65. Approximately 40×10^8 TIC Myr^{-1} becomes transitional interstellar comets (TICs), while 1.4×10^{10} ISO Myr^{-1} interstellar objects (ISOs) over a time interval of 20 Myr. The semi-major axes of these comets are comparable with the distance between Gliese 65 and the Sun. Comets from the system Gliese 65 might reach the solar system in the case that an Oort Cloud-like structure around this star exists. For the remaining systems studied in this work, the rate of TIC production over a time interval of 20 Myr is about 2.1 to 3.8×10^8 TIC Myr^{-1}. This implies that a considerable fraction of interstellar comets reside in the local neighbourhood. Therefore the Sun and its neighbours are visited by interstellar comets originating from other stars. In this way, it is plausible that an interstellar comet cloud exists.

Section 5.1

Introduction

Internal and external perturbations drive the dynamical history and evolution of the population of minor bodies in the solar system, The internal perturbations are due to the instabilities induced by the giant planets on a planetesimal disk at the early stages of the solar system. The external perturbations are due to stars passing near the sun and the Galactic tidal field. These effects play a crucial role in the formation and evolution of the Kuiper belt (e.g., Morbidelli 2005; Brasser & Morbidelli 2013), Oort cloud (e.g., Fouchard et al. 2006; Vokrouhlický et al. 2019) and interstellar comets (e.g., Portegies Zwart et al. 2018; Torres et al. 2019a,b). Close encounters with other stars can disrupt the comets in the Kuiper belt (e.g., Punzo et al. 2014), strip the Oort cloud (e.g. Nordlander et al. 2017; Jílková et al. 2016; Hanse et al. 2016; Bailey & Fabrycky 2019), and create interstellar objects (asteroids/comets). In the early history of the solar system the Sun may have been expelled from its birth cluster due to interaction with the other cluster stars (Portegies Zwart & Jílková 2015; Martínez-Barbosa et al. 2016; Cai et al. 2017). Even though close encounters between the sun and other stars might be rare today, they might have been quite common in the early stages of the solar system, and they will happen in the near future (Torres et al. 2018, 2019a). Studying the effect of multiple interactions with stars and the galactic tidal field can help us to better understand the dynamics of the outer regions of planetary systems with architectures similar to the solar system.

If we assume that other planetary systems undergo similar processes of formation as the solar system, structures like the Kuiper belt and Oort cloud must be common (see, e.g., Potemine 2010; Veras et al. 2014; Caiazzom & Heyl 2017; Baxter et al. 2018; Schwarz et al. 2018; Moro-Martín 2019). Several studies have detected these structures in a variety of primarily low mass stars (see e.g., Vicente & Alves 2005; Kiefer et al. 2014; Pawellek et al. 2014; Welsh & Montgomery 2015; Boyajian et al. 2016; Schwarz et al. 2018). These indicate that reservoirs of comets around stars might be common. Such comet reservoirs will be affected by perturbations due to planets, passing stars, and the Galactic tidal field, which may lead to the production of interstellar comets (Torres et al. 2019a), leading to the extrapolation that interstellar space might by full of such objects.

The discovery of the first interstellar comet, 1I/'Oumuamua (Williams 2017; Meech et al. 2017), and the interstellar comet, 2I/Borisov (Borisov 2019; Guzik et al. 2019), opened up a new era in the study and exploration of the solar system and other planetary systems in our galaxy. The ejection of minor objects from a planetary system, subsequently becoming *sōlī lapidēs* (Portegies Zwart et al. 2018; Torres et al. 2019a,b) or commonly known as interstellar objects or ISOs, is mainly due to the post AGB stellar mass loss and gravitational instability induced by a massive body. This body can be either a nearby planet, a star passing close by or a combination of both (see e.g., Portegies Zwart et al. 2018; Torres et al. 2019a,b; Bannister et al. 2019). Using a catalogue of nearby stars, Torres et al. (2019a) studied the dynamical evolution of comets in the Oort cloud, accounting for perturbations from passing stars and the Galactic tidal field. They found that the cumulative effect of distant stellar encounters and the Galactic tidal field raises the semi-major axis of $\sim 1.2\%$ of the total number of comets in the cloud out to interstellar regions. Such comets becomes transitional interstellar comets (hereinafter TICs) satisfying the condition $e_c \leqslant 1$ and $a_c > a_{EOC}$. Where e_c and a_c are the eccentricity and the semi-major axis of the comet in the cloud and a_{EOC} is the semi-major axis of the exo-Oort cloud (Eq. (5.1)).

Following up on the results of Torres et al. (2019a) in this work we aim to study the formation of TICs around nearby stars (assuming that they have an exo-Oort cloud) to investigate if ISOs from the nearby stars could interact with the solar system. We explore the history of stellar encounters for stars within 3 pc from the Sun, using astrometric data from Gaia DR2 (Gaia Collaboration et al. 2018, 2016). The stars studied are Proxima Centauri, Barnard's star, Gliese 65, Ross 154, and Ross 248. We consider the scenario in which these stars have an exo-Oort cloud and focus on the dynamical evolution of the comets in those clouds due to the stellar encounters and the Galactic tidal field, leading to the production of TICs and ISOs. In Sect. 5.2 we present the closest encounters that each of the nearby stars to the Sun has had in the past 10 Myr and will have in the next 10 Myr. In addition we quantify the change of the velocity produced for the closest stars using the impulse approximation. In Sect. 5.3 we study the dynamical evolution of exo-Oort clouds around the Sun's nearest neighbours under the influence of passing stars and the Galactic tidal field. We analyse the production of TICs and ISOs. Finally, in Sect. 5.4, we present our summary and conclusions.

Section 5.2

Close stellar encounters experienced by the Sun's nearest neighbours

Using the catalogue of nearby stars presented in Torres et al. (2019a) we selected the stars for which we model the exo-Oort clouds from within a 3 pc radius around the Sun at the present time; Proxima Centauri, Barnard's star, Sirius B, GJ 65B, GJ 65A, Ross 154, and Ross 248. The binary system GJ 65 A/B is in a sufficiently tight orbit to be modelled (for simplicity) as one system with a shared exo-Oort cloud. We have chosen to exclude Sirius A and B from the exo-Oort cloud modelling as it uncertain whether a binary hosting an evolved star which has experience significant mass loss will have retained any exo-Oort clouds (circumstellar or circumbinary) that may have existed in the past. However, the effect of Sirius B on the Oort clouds of the 5 systems above is taken into account in our calculations. The stars for which we model the exo-Oort clouds are shown in Fig. 5.1 and Table 5.1. The estimates presented in this work are conservative and based on a small sample of known stars. Therefore this corresponds a lower limit of the total number of Sun's neighbour stars. The catalogue of nearby stars was built using only Gaia DR2 astrometric data, this excludes the well known nearby stars within $\sim$3 pc from the Sun, α Cen A, α Cen B, WISEA J085510.74-071442.5, GJ 406, GJ 411, and Sirius.

The Torres et al. (2019a) catalogue was constructed using the positions, parallaxes, proper motions, and radial velocities from Gaia DR2, and includes additional radial velocities from RAVE-DR5 (Kunder et al. 2017), GALAH DR2 (Buder et al. 2018), LAMOST DR3 (Zhao et al. 2012), APOGEE DR14 (Abolfathi et al. 2018), and XHIP (Anderson & Francis 2012). It contains 14 659 stars and it constitutes an astrometrically clean sample which is incomplete due to the Gaia survey limitations, the upper limit imposed on the distance to the stars in the sample (50 pc), and the strict data-quality filtering from Lindegren et al. (2018). Using Galactocentric Cartesian coordinates we integrated the orbit of the stars in the Torres et al. (2019a) catalogue 10 Myr forwards and backwards in time for a total time of 20 Myr. The orbit integrations were done with the Gala package (Price-Whelan 2017), using an analytic axisymmetric model for the galactic potential, which consists of a spherical nucleus and bulge (Hernquist 1990), a Miyamoto-Nagai disk (Miyamoto & Nagai 1975; Bovy 2015), and a spherical Navarro-Frenk-White (NFW) dark matter halo (Navarro et al.

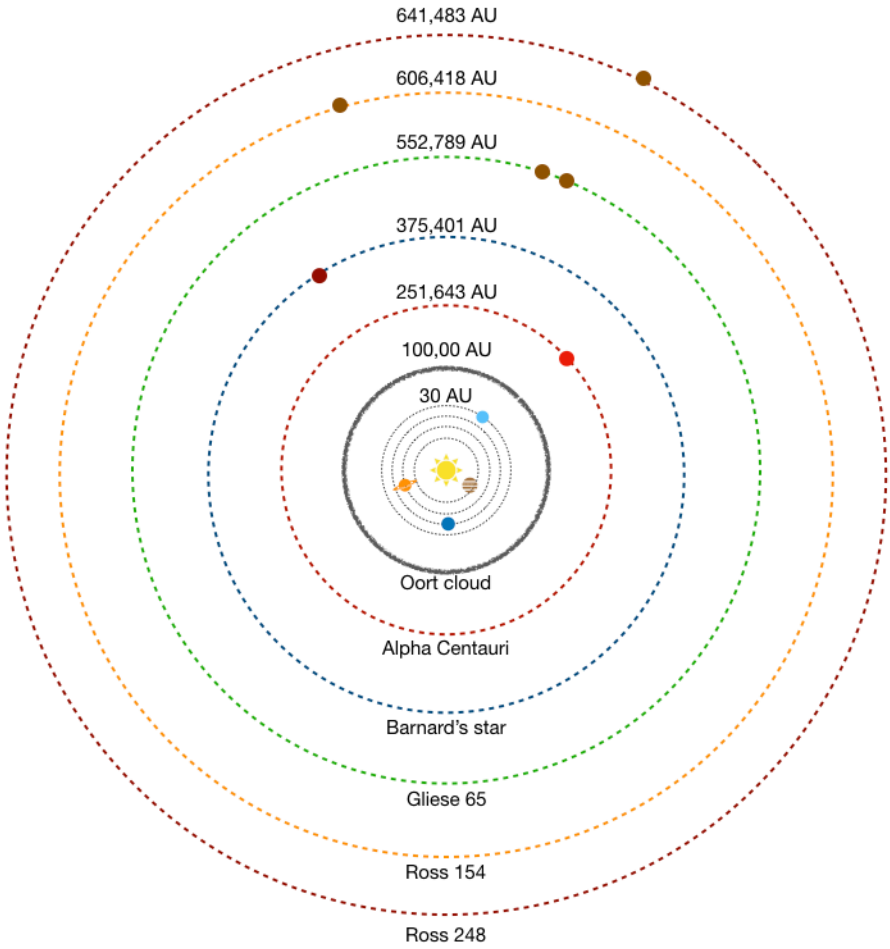

Figure 5.1: Schematic representation of the stars within 650 000 au ($\sim$ 3 pc) from the Sun (not to scale). The inner part of the figure shows the solar system and the Oort cloud. The surrounding rings represent the closest stars to the Sun: Proxima Centauri (red), Barnard's star (blue), Gliese 65 (green), Ross 154 (yellow), and Ross 248 (brown). The distances to the stars are listed at the top of the rings. Coloured dots represents the spectral type of the stars; brown stands for brown dwarfs, red for red dwarfs, and yellow for G stars.

1996). Using a KD-Tree we identified stars from the Torres et al. (2019a) catalogue that approach the stars under study here to within 2.5 pc. The results are listed in Table 5.2. In Fig. 5.2 we show the time and the distance of the closest approach for each close stellar encounter experienced by the stars listed in Table 5.2. On average the nearby systems experience ~ 50 encounters during 20 Myr (third column, Table 5.2).

For the stars within 3 pc from the Sun we calculate the size of the exo-Oort clouds that potentially surround them (Table 5.2). Following the works of Hanse et al. (2016) we scale the outer edge of the exo-Oort cloud to the Hill radius of the parent star in the Galactic potential:

$$\approx a_{\rm OC} \frac{R_*}{R} \left(\frac{M_*}{M} \frac{M_G(R)}{M_G(R_*)} \right)^{1/3} \tag{5.1}$$

where $a_{\rm OC}$ is the semi-major axis of the Oort cloud of the Sun, while R and R_* are the the Galactocentric radii of the Sun and the star, respectively. The terms $M_G(R)$ and $M_G(R_*)$ are the cumulative mass of the Galaxy enclosed within the radius R, and are calculated from our Galactic potential. Considering that the stars listed in Table 5.2 have $R_* \approx R$, Eq. (5.1) can be written as follows:

$$\approx a_{\rm OC} \left(\frac{M_*}{M} \right)^{\frac{1}{3}} . \tag{5.2}$$

To calculate the effect of a nearby star on the comets in an exo-Oort cloud two ingredients are needed; the escape velocity () from the comet's host star, and the change in velocity of the comets () after the interaction. If the final velocity of the comets after the interaction with the passing star is larger than the escape velocity, these will be dislodged from the cloud. The escape velocity (Fig. 5.3) is calculated considering the values for the outer edge of the exo-Oort cloud of each star, calculated using Eq. (5.2) and listed in Table 5.1. Subsequently, using the impulse approximation (Oort 1950; Rickman 1976) we calculate the change of the velocity due to a passing star as:

$$\propto \frac{M_* r_c}{v_* r_h^2} , \tag{5.3}$$

Table 5.1: Stars within 3 pc from the Sun. The first column shows the name of the star, followed by the Gaia DR2 identification, the distance to the Sun, the spectral type (ST), and the mass.

Star	Gaia DR2 ID	*Distance (pc)	ST	Mass (M)
Proxima Centauri	5853498713160606720	1.30	M5	0.122^{a}
Barnard's star	4472832130942575872	1.82	M4	0.144^{b}
Gliese 65	5140693571158739712	2.69	M5	0.202^{c}
Ross 154	4075141768785646848	2.98	M3	0.170^{d}
Ross 248	1926461164913660160	3.16	M6	0.136^{e}

*Distance calculated from Gaia DR2 parallaxes. $^{(a)}$Mann et al. (2015), $^{(b)}$Ribas et al. (2018), $^{(c)}$ Considering the mass of Gliese 65 a and b Delfosse et al. (2000), $^{(d)}$Davison et al. (2015), $^{(e)}$Jenkins et al. (2009).

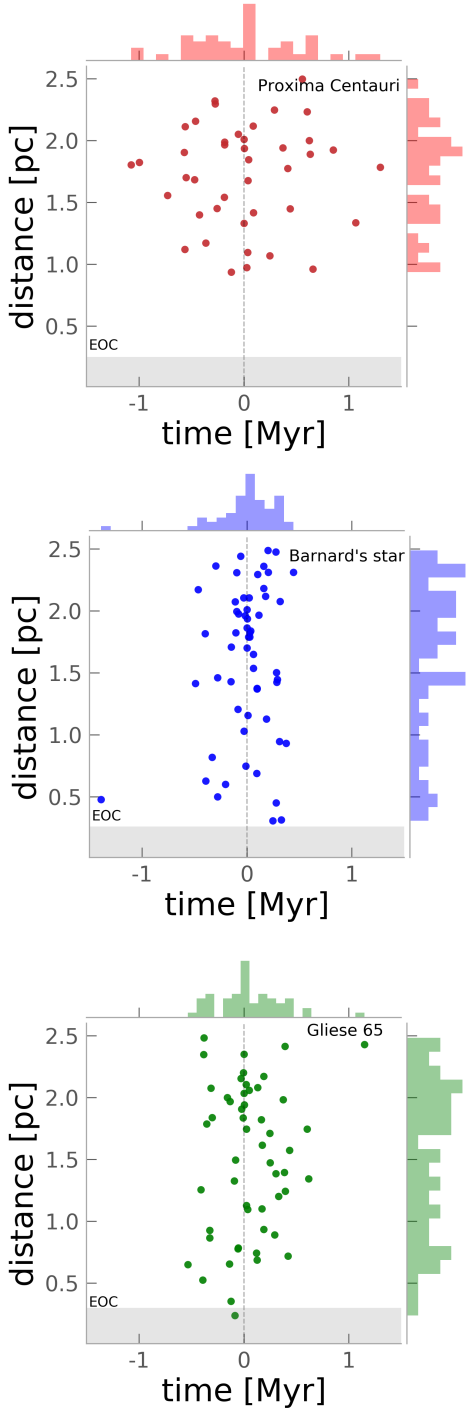

Figure 5.2: Continue...

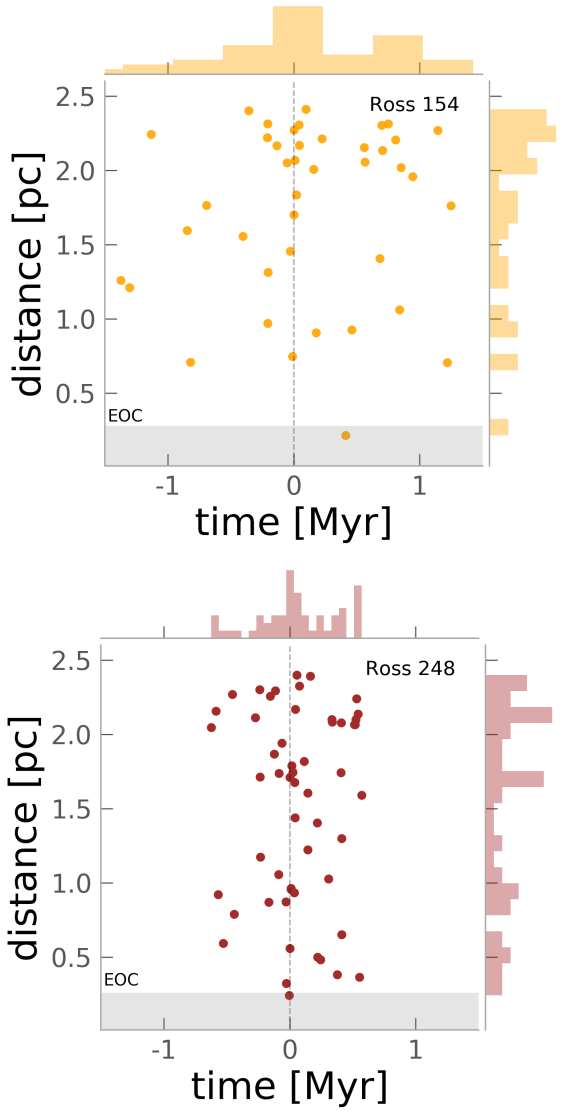

Figure 5.2: Closest approach distance versus the time of closest approach. The top panel (red colours) shows the closest encounters between Proxima Centauri and the stars in the Torres et al. (2019a) catalogue over a time interval of 20 Myr centred on the present. Following by Barnard's star (blue), Gliese 65 (green), Ross 154 (yellow), and Ross 248 (brown). The histograms in each panel represents the marginal distributions in distance and time. The shaded areas represent the boundaries of the outer Oort cloud for each star.

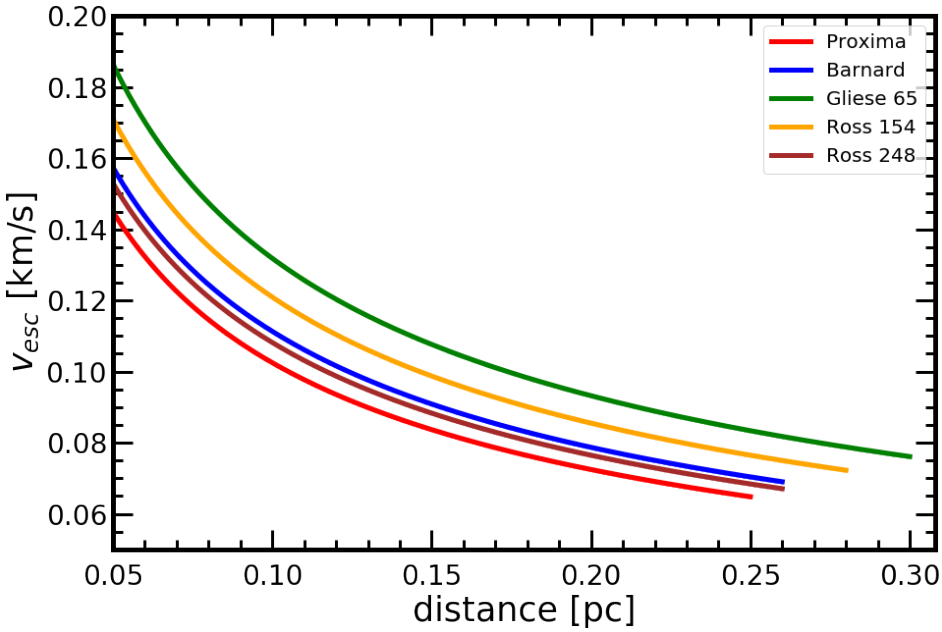

Figure 5.3: Escape velocity as a function of the distance from the star for Proxima Centauri (red), Barnard's star (blue), Gliese 65 (green), Ross 154 (yellow), and Ross 248 (brown).

where M_* and v_* are the mass and velocity of the passing star in and km s^{-1}, respectively. The distance of the exo-comet to its host star is r_c, while r_h is the distance of the host star to the passing star at the point of closest approach. The total change of the velocity induced by the stars passing closest to the solar neighbours studied in this work is listed in the last column of Table 5.2.

In Fig. 5.2 and Table 5.2 we show the closest approach distance and time for each of the Sun's closest neighbours. The limited distance range of the stars in the Torres et al. (2019a) sample only allows us to find close encounters (< 2.5 pc) that occur within ± 1.5 Myr from the present for the total period of integration (± 10 Myr). Here we discuss the effect exclusively due to the impulse imparted to the comets during the close encounters between the stars in Table 5.1 and the stars in the Torres et al. (2019a) catalogue. The full cumulative effect of the encounters and Galactic tidal field are studied in the next section. For the systems discussed below Table 5.2 lists both the circular and the escape velocity at the edge of the exo-Oort

Table 5.2: Stellar encounter statistics for the Sun and its closest neighbours. The first column shows the name of the star followed by the distance and time of the closest approach by another star from the Torres et al. (2019a) catalogue. The fourth column indicates the number of encounters closer than 2.5 pc that each system experiences during 20 Myr, followed by the circular and escape velocity in the (exo-)Oort cloud. Columns seven and eight show the average and the total change of the velocity (Eq. (5.3)) induced by the closest encounters for each star. The last column shows the size of the outer edge of the (exo-)Oort cloud (). The Full list of the stellar encounters for each star in this table can be found online. The encounter statistics for the Sun are taken from Torres et al. (2019a).

Star	d_{ph} (pc)	t_{ph} (Myr)	N_{enc} < 2.5 pc	v_{cir} (km s^{-1})	v_{esc} (km s^{-1})	$\langle \Delta V_\perp \rangle$ (km s^{-1})	$\sum \Delta V_\perp$ (km s^{-1})	EOC (pc)
Sun	0.05	1.28	31	0.092	0.131	4.275e-03	1.325e-01	0.50
Proxima Centauri	0.93	-0.11	40	0.045	0.064	5.929e-05	2.371e-03	0.25
Barnard's star	0.30	0.24	55	0.048	0.069	1.765e-04	1.006e-02	0.26
Gliese 65	0.23	-0.08	51	0.043	0.061	1.846e-04	9.786e-03	0.30
Ross 154	0.21	0.41	45	0.051	0.072	2.244e-04	1.032e-02	0.28
Ross 248	0.24	-0.005	53	0.047	0.067	2.060e-04	1.133e-02	0.26

clouds. Comets in those clouds can be stripped away if their velocity change due to the stellar encounters is at least large enough to bridge the gap between the circular speed and the escape speed.

Proxima Centauri encounters 40 stars that approach to within 2.5 pc over the 20 Myr integration interval (first panel, red dots Fig. 5.2). These close approaches all take place over a $\sim$ 3 Myr time interval which is an artifact of the limited volume from which we draw the stellar encounter candidates. The closest approach to Proxima Centauri is a low mass star at 0.93 pc at -0.11 Myr from the present. The total velocity change for the comets in the exo-Oort cloud of Proxima Centauri due to the close encounters is approximately 2.3×10^{-3} km s^{-1}, on average 5.9×10^{-5} km s^{-1} per encounter. This means that the effect of the close encounters is small and exo-comets around Proxima Centauri will not suffer an important change in their orbital elements, considering that the escape velocity at the edge of its exo-Oort cloud is ~ 0.064 km s^{-1}.

Barnard's star experiences 55 close encounters (second panel, blue dots Fig. 5.2), where the closest encounter will happen in 0.24 Myr from today at the distance of 0.30 pc. The total impulse induced by the stars approaching to within 2.5 pc from Barnard's star generates a total change of the velocity of $\sim 1 \times 10^{-2}$ km s^{-1}, on average 1.7×10^{-4} km s^{-1} per encounter. Although on average the effect of the passing stars is relatively small compared to the escape velocity at the edge of the cloud (0.069 km s^{-1}), the final velocity of the comets in this region after the encounters, will be close to their escape velocity. This implies an important change in their orbital elements.

Gliese 65 has the largest exo-Oort cloud (0.3 pc) among the stars in Table 5.2. Gliese 65 experiences 51 close encounters (Fig. 5.2, third panel, green dots) and two very close encounters. The first one with a red dwarf (~ 0.6) at the edge of its exo-Oort cloud (0.23 pc) which produces a change in the comet velocity of 2.2×10^{-3} km s^{-1}. While the second with a solar type star (~ 1) at a distance of 0.35pc, leading to a change in the comet velocity of 1.8×10^{-3} km s^{-1}. If we considered that the escape velocity is limited by 0.076 km s^{-1}at the edge of the cloud the individual effect of these stars, will not perturb enough the comet to strip them from the cloud. However the orbital elements of the comets will be modify by these encounters.

The total change in the comet velocity induced by the closest encounters is $\sim 9.7 \times 10^{-3}$ km s^{-1}, on average the change of the velocity is around 1.8×10^{-4} km s^{-1} per encounter.

Ross 154 has the second largest exo-Oort cloud (0.28 pc) among the stars in Table 5.2. Ross 154 will face a close encounter with a solar-type star (~ 1.1) passing at a distance of 0.21 pc (through the exo-Oort cloud) in 0.41 Myr from today. The change of the velocity produced by this star is approximately 5.5×10^{-3} km s^{-1}. This means a comet at the edge of the cloud where the escape velocity is around 0.07 km s^{-1} will not be stripped from the exo-Oort cloud due to this encounter, but its orbital elements will change. The total change induced by the 45 stellar encounters (see Fig. 5.2, fourth panel, yellow dots) is of the order of 1.03×10^{-2} km s^{-1}, on average of 2.2×10^{-4} km s^{-1} per encounter.

Ross 248 experiences 53 encounters (Fig. 5.2, fifth panel, brown dots), including a close encounter with an M-dwarf with a mass of 0.5 passing at 0.24 pc (just outside its exo-Oort cloud of which the edge is at 0.26 pc). This close encounter produces a change in the velocity of approximately 1.3×10^{-3} km s^{-1}in comet at the edge of the Ross 248 exo-Oort cloud. This change is not enough to strip the comet from the cloud but it is enough to perturb their orbits. The rest of the encounters do not provide a considerable effect on the cloud. On average the close encounters with Ross 248 produce a change of the velocity of $\sim 2.06 \times 10^{-4}$ km s^{-1} per encounter for a total change of $\sim 1.13 \times 10^{-2}$ km s^{-1}.

The effect of the close stellar encounters on the systems studied here is small, the total change of the comet velocities due to the passing stars ranges from $\sim 2.3 \times 10^{-3}$ to $\sim 1.1 \times 10^{-2}$ km s^{-1}. The escape velocity for these systems ranges from 0.061 to 0.076 km s^{-1}, while the circular velocities at the edge of the exo-Oort clouds range from 0.045 to 0.051 km s^{-1} (Fig. 5.2, Table 5.2). This means that the final velocity of the comets after the encounters are not sufficiently large for them to escape the systems. The systems Gliese 65, Barnard's star, Ross 154, and Ross 248 are the most perturbed systems with final velocities just below their escape velocity at the edge of the cloud. For the system Proxima Centauri comets will not suffer an important change and their orbits and they will remain relatively stable after the encounters.

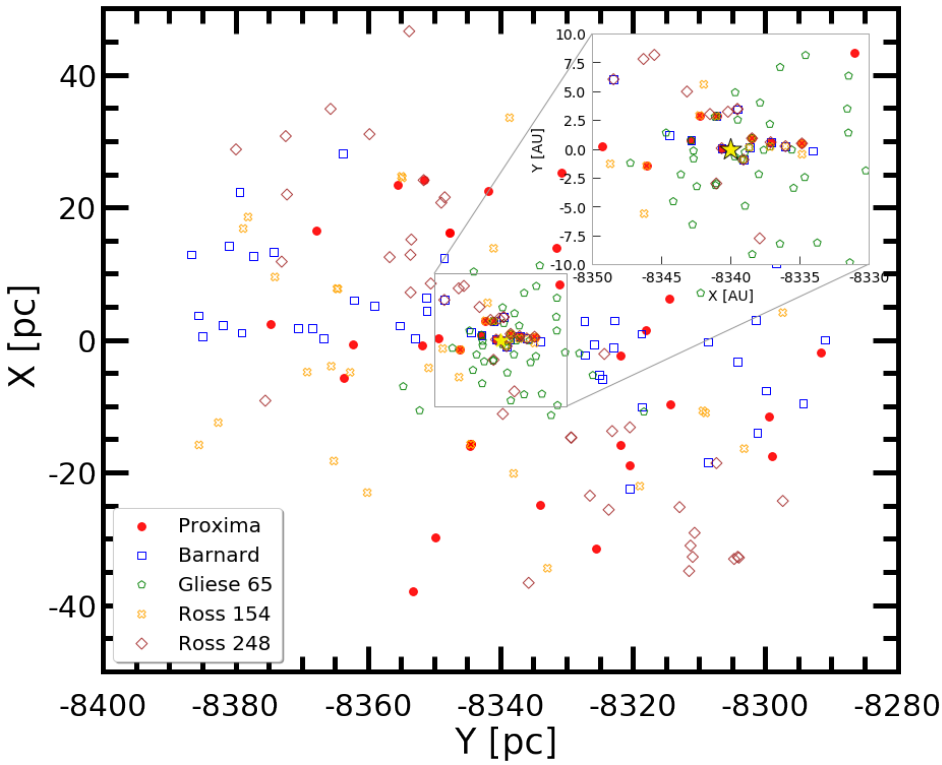

Figure 5.4: Galactocentric coordinates of the present day positions of the stars that have made or will make close approaches to the systems Proxima Centauri (red dots), Barnard's star (blue squares), Gliese 65 (green pentagons), Ross 154 (yellow cruces), and Ross 248 (brown diamonds). The inner plot represents a zoom-in of the central area, where the big yellow star represents the Sun and the mentioned systems.

The low mass of perturbers (0.1–1) as well as the relatively large distance of closest approach (as compared to the exo-Oort cloud sizes) explains the small effect produced by the flybys. It is interesting to point out that even though the closest systems to the Sun are not heavily perturbed by their nearest neighbour stars, the local solar neighbourhood is crowded as shown in Fig. 5.4 where the current positions of all the stars interacting with the systems in Table 5.2 are shown. This indicates that the journey through interstellar space of the comets dislodged from their host system will be determined by the stars in the solar neighbourhood.

The results presented in this section gave us a general picture of the encounter history of the Sun's nearest neighbours and the effects thereof on

the comets in an Oort cloud like structure. However, to have more accurate information about the dynamics of the comets in the exo-Oort clouds it is necessary to integrate their orbits in a Galactic potential, accounting not only for the effect of single stellar encounters but studying the cumulative effect of the encounters and the Galactic tidal field. This is the topic of the next section.

Section 5.3

Dynamical evolution of exo-Oort clouds of the Sun's neighbour stars

Torres et al. (2019a) studied the cumulative effects on the Sun's Oort cloud due to the flybys of nearby stars and the Galactic tidal field over a period of 20 Myr (centred on the present time). They found that relatively close encounters (< 2.5 pc) and the tides form the Galaxy considerably perturbed the outer regions of the Oort cloud, turning about 1.2% of the comets into transitional interstellar comets (TICs). Motivated by these results we investigate the dynamics of the Oort Cloud-like structures around some of the Sun's nearest neighbours (Table 5.1). We first assume that these stars posses an Oort cloud-like structure. Following the method of Torres et al. (2019a) we add an artificial isotropic cloud of comets to each star with $10\,000$ test particles each. We limited the size of the Oort cloud according to Eq. (5.2) for each star in Table 5.2. The exo-Oort clouds are constructed in such a way that the distribution of the particles is symmetric and isotropic, and they follow a uniform distribution in the orbital elements $\cos i$ (inclination), ω (argument of periapsis), Ω (longitude of the ascending node), and M (mean anomaly). The initial eccentricities, e, are selected with a probability density distribution $p(e) \propto e$. The semi-major axes, a, are distributed proportional to $a^{-1.5}$ over the range 3×10^3 au and the outer edge of each cloud. To ensure a thermalised Oort cloud (e.g. Duncan et al. (1987); Dybczyński (2002); Rickman et al. (2008)) we used a radial density profile of $r^{-3.5}$ (where r is the distance between the comets and the star).

Our numerical simulations rely on the Astrophysical Multi-purpose Software Environment, AMUSE (Portegies Zwart et al. 2009; Pelupessy et al. 2013; Portegies Zwart et al. 2013b; Portegies Zwart & McMillan 2018) and the GPU-accelerated direct N-body code ABIE (Roa et al. in press, Cai et al. in preparation) with a fifteenth-order Gauss-Radau integrator (Everhart 1985) optimised for close encounters. We investigate the effect of

stellar encounters and the galactic tidal field on the exo-Oort cloud of each system in Table 5.1. To achieve that we couple ABIE and the Gala (Price-Whelan 2017) package in such a way that ABIE advances the positions of the exo-Oort cloud particles and Gala calculates the accelerations on each particle due to the Galactic tidal field, based on the positions provided by ABIE. The calculated accelerations are subsequently inserted into the Gauss-Radau integrator in ABIE as additional forces.

The stars listed in Table 5.1 are primarily brown dwarfs, with masses around 0.1 . This means that the outer edge of their exo-Oort clouds extends to about 0.2 pc from the host star. For this size of exo-Oort cloud the contribution of the Galactic tidal filed is rather small and therefore the effect on the comets at the edge will be minimal (Torres et al. (2019a)). Therefore, the predominant perturbation is due to the relatively close passing stars. In Fig. 5.5 and Fig. 5.6, we show the change of the perihelion as a function of the final semi-major axis and eccentricity for the particles in the exo-Oort cloud for each system in Table 5.1. For each individual system we find the following results.

Note that below we present the number of TICs or ISO produced in two ways; as the percentage of the $10\,000$ simulated particles and as a rate of TIC/ISO production per Myr which is found be scaling the simulated exo-Oort clouds to the number of comets estimated to exist in the solar system Oort cloud ($\sim 10^{12}$ commets, Morbidelli et al. 2005).

Proxima Centauri The effect of the Galactic tidal field and stellar encounters on the exo-Oort cloud of Proxima Centauri is relatively small, with the closest approach of another star happening at a distance of 0.93 pc. Nevertheless a small fraction, ~ 0.42% of the initial comets in the cloud are turned into TICs after 20 Myr (Fig. 5.5 and Fig. 5.6). The production rate of TICs of Proxima Centauri during those 20 Myr is $\sim 2.1 \times 10^8$ TIC Myr^{-1}. The change of perihelion for the particles in the cloud is up to $10\,000$ au for the particles with initial semi-major axes between $47\,000$ and $51\,500$ au, which is the most disturbed region of the cloud. The inner parts of the cloud are nearly unperturbed. In Fig. 5.5 yellow particles represent the change of the perihelion as a function of the final semi-major axis for the TICs originating from the solar system (compare to Fig. 12 in Torres et al. 2019a). As can be seen in Fig. 5.5, due to its proximity to the Sun the Hill sphere of Proxima Centauri overlaps with the simulated TICs originating from the solar system and we may thus speculate about comets originating from the

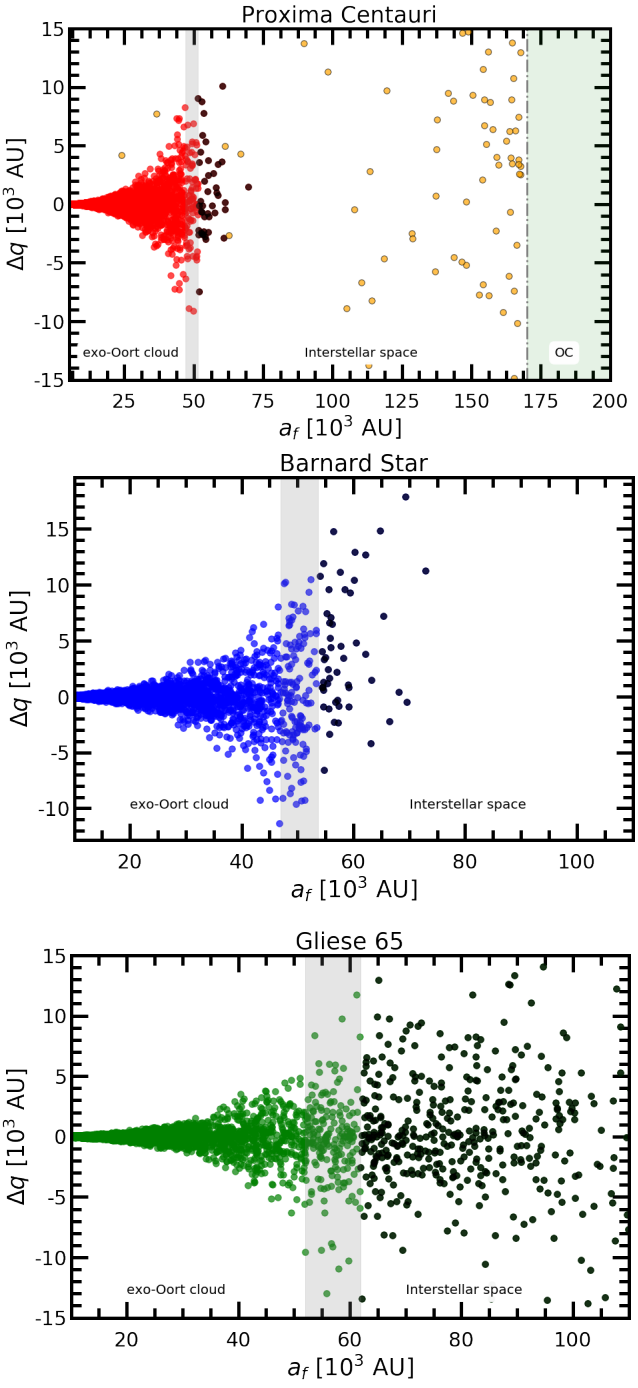

Figure 5.5: Continue...

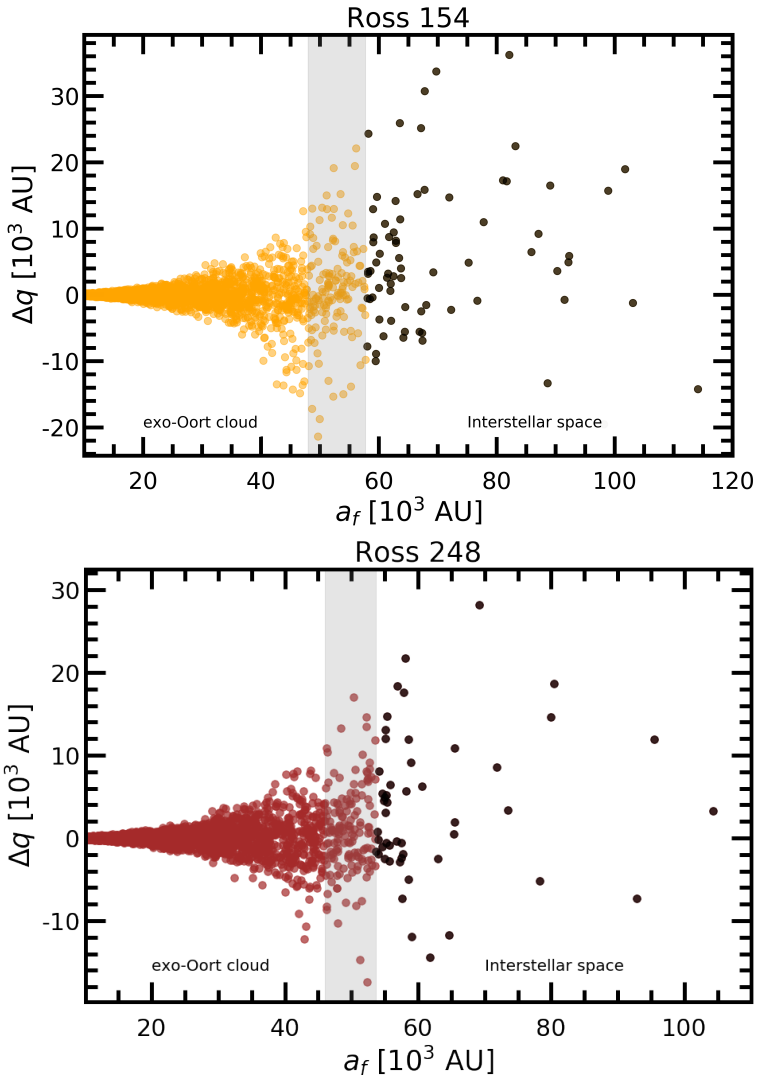

Figure 5.5: Mean periapse changes as a function of the semi-major axis of the particles in the exo-Oort clouds. The grey area corresponds to the region of the initial position of the particles ejected, represented as black dots. The first panel corresponds to Proxima Centauri (red), followed by the systems Barnard's star (blue), Gliese 65 (green), Ross 154 (yellow), and Ross 248 (brown).

solar system entering the Proxima Centauri system. Due to the small perturbations of the exo-Oort cloud of Proxima the opposite does not happen. However, our calculations are limited by the incompleteness of our catalogue of stars in the solar neighbourhood. For a complete and accurate sample of star the production of TICs will naturally increase, which also increases the chances of our solar system capturing a comet from Proxima Centauri. Note that Proxima is know to host a planet (Anglada-Escudé et al. 2016) which makes the existence of an exo-Oort cloud in this system plausible (see also Schwarz et al. 2018).

Barnard's star With 55 encounters, the encounter history of Barnard's star is the most eventful among the closest stars to the Sun. The cumulative effect of the passing stars and in particular the close encounter at 0.30 pc (near the edge of the exo-Oort cloud) raises the semi-major axis and eccentricities of about 0.52% of the total comets in the Oort cloud of Barnard's star becoming TICs. This leads to production rate of TICs during 20 Myr is $\sim 2.6 \times 10^8$ TIC Myr^{-1}. The change in the perihelion of the particles with final semi-major axes between $20\,000$ and $40\,000$ au is up to $5\,000$ au, and for the particles with initial semi-major axes between $47\,000$ and $53\,000$ au the change is up to almost $20\,000$ au (Fig. 5.5). Even though the change in the eccentricity is rather small (Fig. 5.6) future perturbations may lead to the stripping of more particles from the edge of the cloud. The close encounters found in this work are restricted to 3 Myr, a longer window will only increase the perturbations in the system. The possibility of the existence of an exo-Oort cloud around Barnard's star is very high if we consider that there are indications of an exoplanet (super-earth) orbiting the star (Ribas et al. 2018) and that the formation and evolution of exo-comets are linked to the formation and evolution of planets.

Gliese 65 Among the stars listed in Table 5.1 Gliese 65 is the most perturbed system. The change in the perihelion of the particles is around $15,000$ au variation for the region with $52\,000 < a_f < 61\,870$ au. For the inner part of the system ($a_f < 30,000$ au) the change is minimal (Fig. 5.5), and the comets remain in stable orbits. The outer most part of the cloud ($50\,000 < a_f < 61\,870$ au) is heavily perturbed, mainly by the close encounter with a red dwarf with mass of ~ 0.6 at 0.23 pc, a solar-type star with mass of 1 at 0.35 pc, and the Galactic tidal field. The combined effect of the 51 encounters and the tides from the galaxy leads to the ejection

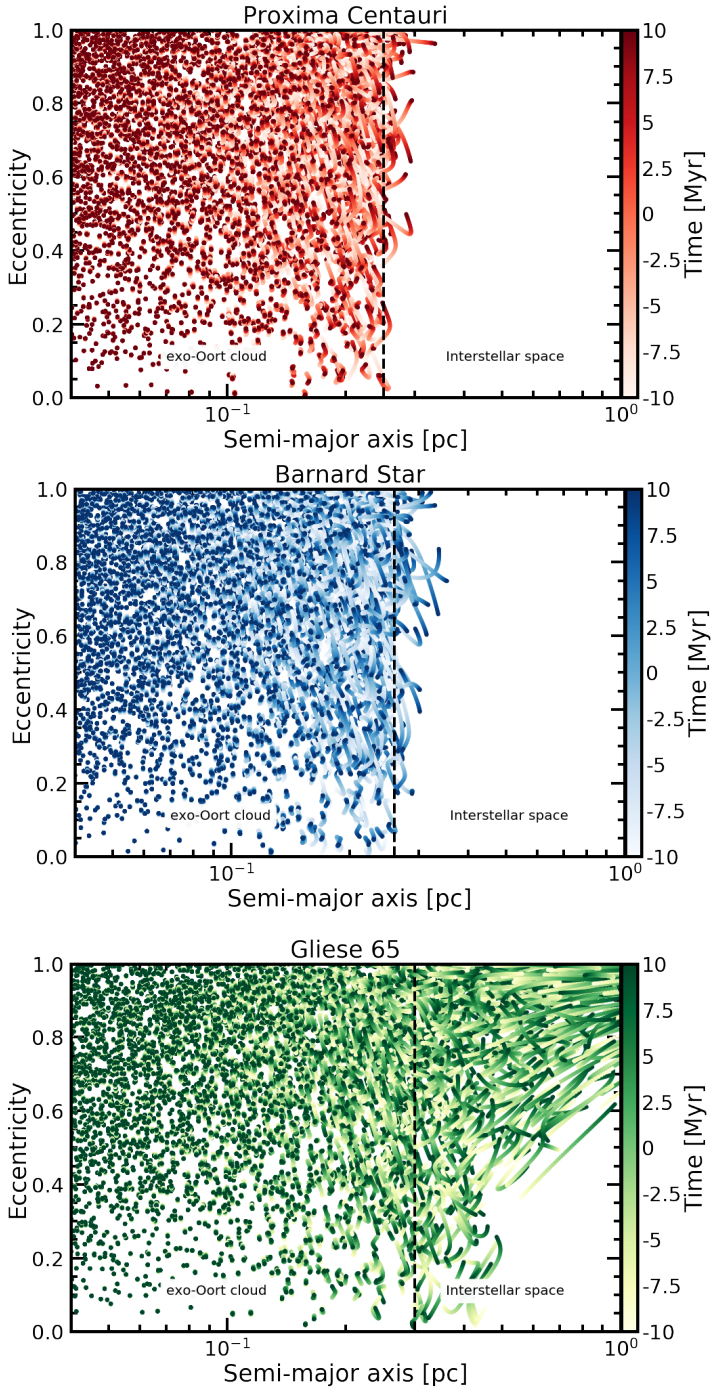

Figure 5.6: Continue...

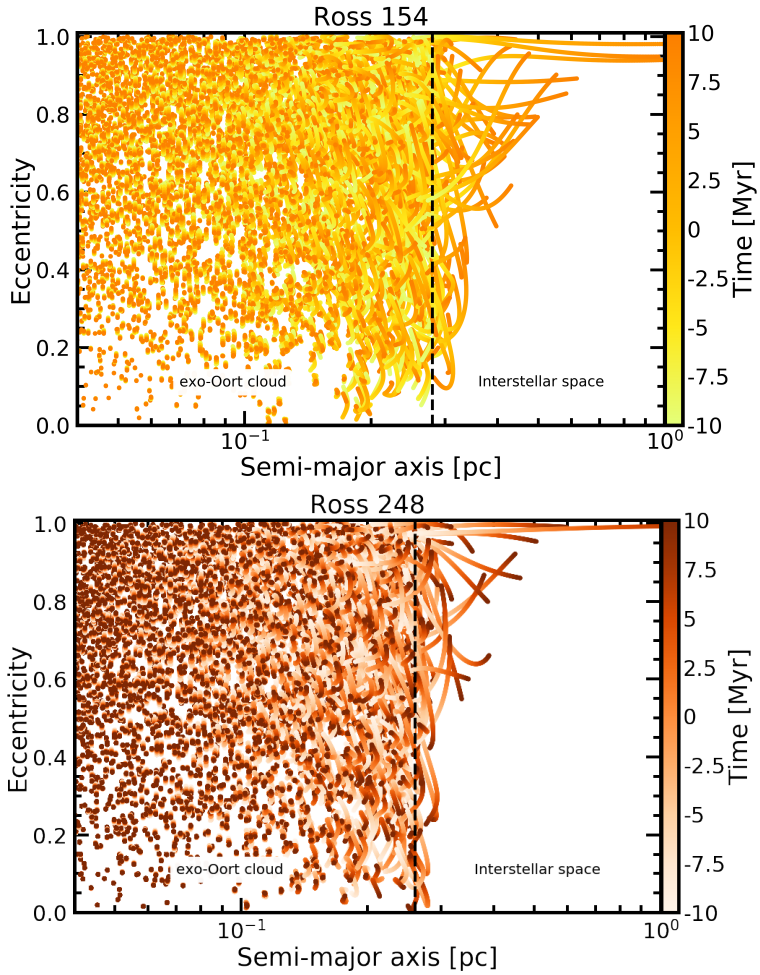

Figure 5.6: Orbital evolution of the particles in the exo-Oort cloud for a period of 20 Myr. First panel corresponds to Proxima Centauri (red), followed by the systems Barnard's star (blue), Gliese 65 (green), Ross 154 (yellow), and Ross 248 (brown).

of about 28.78% of the total number of comets in the cloud. Additionally, $\sim 7.98\%$ of the remaining comets become TICs, with semi-major axis between $\sim 6.1 \times 10^4$ to $\sim 2 \times 10^6$ au. This means that TICs or ISOs from Gliese 65 might reach the solar system if we considered that Gliese 65 is 5.5×10^5 au from the Sun. The production rate of TICs and ISOs of Gliese 65 during 20 Myr are $\sim 40 \times 10^8$ TIC Myr^{-1} and 1.4×10^{10} ISO Myr^{-1}. The analytic calculation in Sect. 5.2, showed that the effect of passing stars on the comets in the exo-Oort cloud of Gliese 65 is limited. However, when using a detailed N-body calculations and particularly accounting for the cumulative effect of passing stars and the Galactic tidal filed shows that the cloud is heavily perturbed. The discrepancy of the results is a clear example of the limitations of using a simple analytic model such as the impulse approximation (Eq. (5.3)). Therefore comparing analytic models with detailed numerical simulations will lead to a more robust conclusion of the results.

Ross 154 This is the second most perturbed system among those listed in Table 5.1, with one close encounter at 0.21 pc (0.41 Myr from today, passing through the exo-Oort cloud) and 45 encounters over 20 Myr. Ross 154 also possesses the second largest exo-Oort cloud among the systems studied in this work, with its edge at 0.28 pc. Particularly the particles with final semi-major axes between $48\,000$ and $57\,750$ au are heavily perturbed, with perihelion changes up to $\sim 34\,000$ au. Around 0.77% of the comets in this region become TICs, with future encounters further increasing their semi-major axis. Around 7% of the TICs reaches $\sim 400\,000$ au, while the rest acquires semi-major axes between $60\,000$ and $120\,000$ au. In the inner part of the cloud ($a_f = 2000$–$30\,000$ au), the particles remain stable with a small variation in their orbital elements (Fig. 5.5 and Fig. 5.6). The TIC production rate of Ross 154 in 20 Myr is $\sim 3.85 \times 10^8$ TIC Myr^{-1}. Considering that our simulations are limited to a 20 Myr time interval, if we let the system evolved for more time the production of TICs will increase (due to more stellar encounters and longer action of the Galactic tidal field) and eventually the particles with largeest semi-major axis will become interstellar comets.

Ross 248 The encounter history of this system is second in terms of number of encounters, with 53 encounters in 20 Myr and one close encounter at 0.24 pc at the edge of its exo-Oort cloud. The perihelion of

the particles within $46,000 < a_f < 53\,000$ au changes by up to $30\,000$ au (Fig. 5.5), while the eccentricities in the same region change considerably over time (Fig. 5.6). The production of TICs is comparable with to the case of Barnard's star with 0.52% of the initial comets transformed to TICs and rate of $\sim 2.6 \times 10^8$ TIC Myr^{-1}. However, the TICs from Ross 248 are considerably more perturbed primarily because of its close encounter with an M-dwarf at the edge of the cloud. Around 13% of the TICs acquired semi-major axes larger than $80\,000$ au, while the rest ranges from $52\,000$ to $80\,000$ au. Only 0.01% of the particles in the cloud become hyperbolic. The perturbations due to the Galactic tidal field and the stellar encounters do not change the dynamics of the inner regions of the cloud.

Overall the effect of the stellar flybys and the Galactic tidal field on the Sun's neighbours is relatively large, considering that all the stars studied are M-dwarfs and therefore their exo-Oort cloud is more compact (within 0.2 and 0.3 pc). In this way, the contribution of the Galactic tidal field is rather small and therefore the most dominant perturbation are the close encounters. The most perturbed systems in our simulations are Gliese 65, Ross 154, Ross 248 and Barnard's star primarily due to a very close encounter with a star passing through their exo-Oort cloud regions.

The total effect on these stars, is reflected in the production rate of TICs and ISOs. For Gliese 65 these rates are about 40×10^8 TIC Myr^{-1} and 1.4×10^{10} ISO Myr^{-1}. Approximately 0.77% of the comets in the Oort cloud of Ross 154 become TICs having a production rate of 3.85×10^{10} TIC Myr^{-1}, which semi-major extends up to $400\,000$ au. For the systems Ross 248 and Barnard's star, the production rate of TICs is the same ($\sim 2.6 \times 10^8$ TIC Myr^{-1}), but the semi-major of the TICs goes up to $200\,000$ au for Ross 248 and $80\,000$ au for Barnard's star. Even though Barnard's star produces the same fraction of TICs as Ross 248, the perturbation of its nearby stars is least strong. This is mainly because the closest encounter with Barnard's star is a brown dwarf, which perturbation is just strong enough to perturbed the comets at the edge of its exo-Oort cloud, but is not strong enough to dislodge the comets.

Finally, one of the most interesting systems in our list is the closest star to the Sun, Proxima Centauri. The encounter history of Proxima is the least eventful in our list, however due to encounters with relatively high mass stars, including the Sun, the production rate of TICs is relatively high ($\sim 2.1 \times 10^8$ TIC Myr^{-1}). We speculate that a small fraction of the TICs from our solar system (~ 5%) will enter the exo-Oort regions of Proxima.

The effect of Galactic tidal field on the stars studied here is limited mainly because on average these M-dwarfs posses small exo-Oort clouds that extend only up to 0.25 pc. Therefore the most prominent perturbation that these stars will suffer is due to the passing stars. Because our list of perturbing stars is incomplete the number of stars perturbing these systems is expected to be higher (see Bailer-Jones et al. 2018). This means that the number of TICs as well as interstellar comets will be higher than estimated here.

5.3.1 TICs/ISOs in the solar neighbourhood

Studying the orbits of interstellar comets can help us to understand the dynamical evolution of the planetary system from which the ISO originated. For the nearby stars to the Sun studied in this work (Table 5.1), Gliese 65 is the most perturbed system. After 20 Myrs and two very close encounters, 7.98% of the total comets in the cloud become TICs, while 28.78% are ejected to the interstellar space. Ross 154 is the system which produces the second largest number of TICs, approximately 0.77% of the total number of comets after 20 Myr. Follow by Ross 248 and Barnard's star with 0.52%, and finally Proxima Centauri with 0.40% (Table 5.3). The dynamical evolution of TICs will be dominated by nearby stars and the Galactic tidal field. As time passes, TICs will face more stellar encounters and particularly the effect of the Galactic tidal field will affect their orbit and they will be dialogued from their host systems becoming ISOs.

For the stars studied here, TICs from *Barnard's star* posses the highest relative velocity to the Sun after 10 Myr, with an average of 32.22 km/s (Fig. 5.7). The variation, in their velocity, is small $\sim$32.2-33.2 km/s. The second system with high relative velocity to the Sun after 10 Myr, is *Gliese 65*, with an average velocity of 24.14 km/s, and with velocities ranging from approximately 24.13-24.14 km/s. The third and last system with high relative velocity is *Ross 248* with an average velocity of 20.63 km/s and a variation going from 20.62-20.64 km/s. The systems *Proxima Centauri* and *Ross 154* have small velocities with respect to the Sun after 10 Myr, ranging from 7.32-7.72 km/s and 3.930-3.942 km/s respectively. The small variation of the TICs relative velocity is expected because the TICs are leaving the system gradually and their velocity is thus dominated by the velocity of the host star.

The small change in velocity is enough to allow the comets to leave the Hill sphere of the host stars and is mainly induced by the cumulative

Table 5.3: Production of TICs and ISOs from the nearby stars to the Sun. The first column shows the name of the star, followed by the percentage of the total comets in the exo-Oort clouds that becomes TIC or ISO. The last column represents the average of the total relative velocity of the TICs respects to the Sun for each star after 10 Myr of orbital integration.

Star	TIC (%)	ISO (%)	$\langle v_{rel} \rangle$ (km s^{-1})
Proxima Centauri	0.40	0	7.22
Barnard's star	0.52	0	32.22
Gliese 65	7.98	28.78	24.14
Ross 154	0.52	0	3.93
Ross 248	0.77	0.01	20.63

effect of the close encounters that each system faced over the 20 Myr of integration. If we compare the relative velocity of the TICs in Table 5.3 with 1I/'Oumuamua ($\sim$26.3 km/s, Meech et al. 2017) and 2I/Borisov (32.2 km/s, Borisov 2019; Guzik et al. 2019) their velocities match with the TICs from *Gliese 65* and *Barnard's star* respectively. This does not imply that 1I/'Oumuamua and 2I/Borisov came from those stars. However, if we considered that ISOs have small velocity when leaving their systems (Torres et al. 2019b; Hands et al. 2019). The relative velocity of planetary systems can be used to constrain the velocity of the ejected object. For the future detections of ISOs, matching the relative velocity with those stars in the solar neighbourhood and performing backward orbital integration (e.g., Portegies Zwart et al. 2018) will serve as constrain of their possible origin.

Section 5.4

Summary and Conclusions

Following the results and methods of Torres et al. (2019a), in this paper, we explored the dynamical evolution of exo-Oort clouds around the nearest stars to the Sun. We selected the stars within 3 pc from the Sun, which we assumed to possess an Oort cloud-like structure and with accurate astrometric data from Gaia DR2. The selected systems are: Proxima Centauri, Barnard's star, Gliese 65, Ross 154, and Ross 248. In Sect. 5.2, we calculated the number of stellar encounters that each of the systems faced in

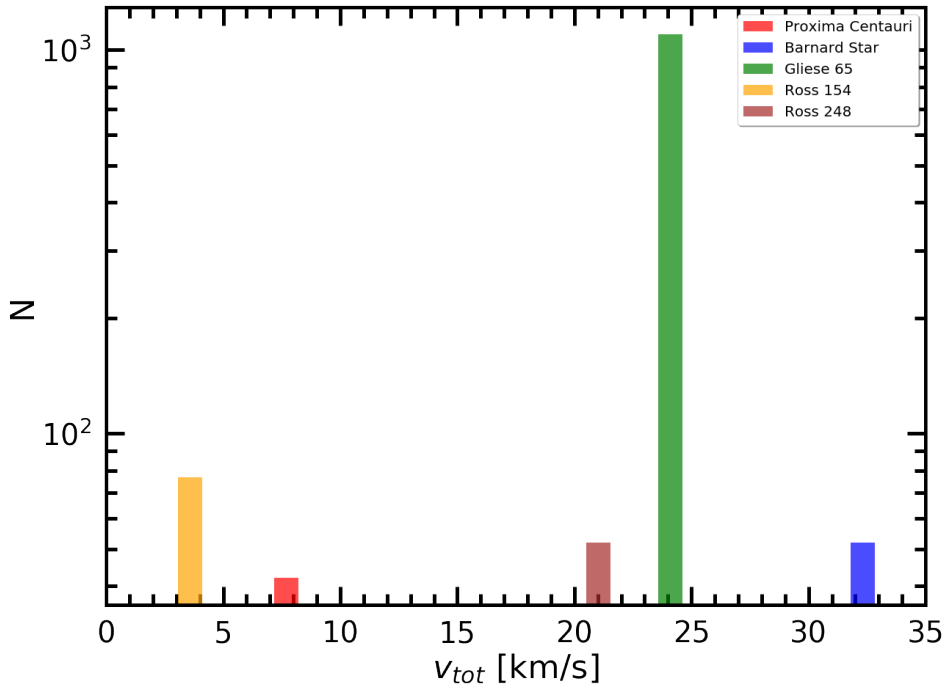

Figure 5.7: Histogram of the relative velocity of the TICs from the stars in Table 5.1 respect to the Sun. Colour bars corresponds to the systems Proxima Centauri (red), followed by the systems Barnard's star (blue), Gliese 65 (green), Ross 154 (yellow), and Ross 248 (brown).

the past 10 Myr and would encounter in the next 10 Myr. We find that on average, these systems experience around 40-55 encounters in 20 Myr.

Using the impulse approximation (Eq. (5.3)), we calculated the change of the velocity induced by a passing star to a comet in an exo-Oort cloud. We find that the most perturbed systems due to a close encounters are Gliese 65, Ross 154, Ross 248, and Barnard's star. Their final velocities are below the escape velocity at the edge of their exo-Oort cloud (Table 5.2). For Proxima Centauri the effect of the passing stars do not represent an essential change in the velocity of their comets.

To have a complete study of the effect of passing stars on the Sun's neighbour stars, in Sect. 5.3 we studied the dynamical evolution of the comets in an exo-Oort cloud. We included the cumulative effect of passing stars within 2.5 pc from each system and the Galactic tidal field. Using the encounter history of the nearby stars to the Sun (Table 5.2), we inte-

grated the orbits of the comets for 20 Myr (10 Myr in the past, 10 Myr in the future). For the five stars studied in this work (Table 5.1), Gliese 65, is the most perturbed system. Gliese 65 is a binary system of which Oort Cloud extends up to 0.3 pc. It faces 51 encounters in 20 Myr, having two very close encounters at a distance of 0.23 and 0.35 pc. The combined effect of all close encounters (primarily the two closest) and the tides from the Galaxy, leads to a production rate of TICs and ISOs of about 40×10^8 TIC Myr^{-1} and 1.4×10^{10} ISO Myr^{-1} over a time interval of 20 Myr. The semi-major axis of the TICs from Gliese 65 ranges from $\sim 6.1 \times 10^4$ to $\sim 2 \times 10^6$ au. This implies that TICs or ISOs from Gliese 65 might reach the solar system's Oort cloud whose is located $\sim 5.5 \times 10^5$ au away.

Ross 154, faced a close encounter with a G-star at 0.21 pc (at the edge of its exo-Oort cloud) and 45 encounters within 2.5 pc. These encounters and the effects from the tides of the Galaxy form approximately 3.8×10^8 TIC Myr^{-1}. The follow most perturbed system are Ross 248, Barnard's star, and Proxima Centauri. The systems Barnard's star and Ross 248 faced similar encounter histories (55, and 53 encounters), which perturbations lead to the formation of $\sim 2.6 \times 10^8$ TIC Myr^{-1} for both cases over 20 Myr. Nevertheless, the perturbation is larger in Ross 248, due to a close encounter at 0.24 pc (inside of its exo-Oort cloud). This is reflected in the larger semi-major axis of the TICs compared to the ones in Barnard's star (Fig. 5.6). Finally, Proxima Centauri faces 40 encounters during 20 Myr, which together with the tides from the Galaxy leads production rate of $\sim 2.1 \times 10^8$ TIC Myr^{-1}. Due to its proximity to the Sun, the exo-Oort cloud of Proxima Centauri overlaps with $\sim$5% of the TICs originating from the solar system (Fig. 12 in Torres et al. 2019a). Therefore we may speculate that objects coming from the solar system enter Proxima Centauri. Due to the small perturbations of the exo-Oort cloud of Proxima, the opposite does not happen in our calculations.

Overall, the effect of passing stars dominates over the tides from the Galaxy. The impact of the Galactic tidal field is too weak on the short time scale studied here, to affect the orbital elements of the comets in the exo-Oort cloud. Because of the small size of the exo-Oort cloud (approximately half of the Oort cloud of the Sun), and the position of the stars in the Galactic plane. However, it is the combined effect of the Galactic tidal field and stellar encounters which shaped the edge of the exo-Oort clouds studied in this work. It is important to stress that estimates presented in this work are conservative and based on a small sample of known stars. The production rates of TIC scale with the total number of comets in the Oort cloud

for all the systems presented in this work is approximately of order 10^8 TIC Myr^{-1} over a time interval of 20 Myr. A complete sample of nearby stars will naturally increase the number of TICs and ISOs in the local solar neighbourhood. This implies that the nearby systems with an exo-Oort cloud including the solar system might get constantly polluted by interstellar comets. Therefore an interstellar cloud of comets is very plausible.

Acknowledgements ST expresses his gratitude to the Mexican National Council for Science and Technology (CONACYT) for the grant #291004-410 780; to Leiden Observatory for the unconditional support; and to Maxwell Cai and Ylva Götberg, for the discussions and comments on the manuscript. This work has made use of data from the European Space Agency (ESA) mission Gaia (https://www.cosmos.esa.int/gaia), processed by the Gaia Data Processing and Analysis Consortium (DPAC, https://www.cosmos.esa.int/web/gaia/dpac/consortium). Funding for the DPAC has been provided by national institutions, in particular the institutions participating in the Gaia Multilateral Agreement. This work was carried out on the Dutch national e-infrastructure with the use of *Cartesius* the Dutch national supercomputer and the support of SURF Cooperative.